PROPAGATION IN CURVED MULTIMODE CLADDED FIBRES

W.A.Gambling, D.N.Payne and H.Matsumura
Department of Electronics
University of Southampton
Southampton SO9 5NH, U.K.

SUMMARY

An analysis is given of coupling between modes in a curved, cylindrical, multimode optical fibre and very simple forms for the coupling coefficients are obtained. In general $HE_{l,m}$ modes couple strongly to those designated $HE_{2,m}$; $HE_{2,m-1}$; $TE_{0,m}$; and $TE_{0,m-1}$. In particular the HE_{11} mode couples almost exclusively to the HE_{21} and TE_{01} modes and coupling to higher modes can, to first order, be neglected. The degree of mode conversion is largely restricted to a periodic exchange of energy, between these few modes, along the length of the fibre with a periodicity which can be less than 1mm. Excellent agreement is obtained between theory and experiment. This form of quasi-single-mode operation is reflected in very low values of pulse dispersion but is very sensitive to stress in the fibre. The significance of these results in terms of mode conversion is discussed.

1. INTRODUCTION

It was originally expected that propagation in long optical fibres would be dominated by scattering due to imperfections in the core and at the core/cladding interface. However it has been shown possible to make fibres very accurately (Payne, D.N. and Gambling,W.A. 1973), for example having a change in outside diameter of less than 1μm in 100μm over lengths of several hundred metres, and in this case their behaviour can become similar to that of an overmoded waveguide. However, in solid-core fibres, in addition to geometrical imperfections, there is also the possibility of optical inhomogeneities due to stress. Nevertheless many of the features of the observed propagation effects, such as the time dispersion of short optical pulses, can be explained in terms of a simple ray model (Gambling,W.A., Dakin,J.P., Payne,D.N. and Sunak,H. 1972), but the mechanism of the residual mode scattering is not understood.

Liquid-core fibres have the advantage that not only are they available with very low loss (<6dB/km) but stress effects in the core are absent and a more fundamental study of propagation and mode conversion is possible. Early measurements showed a strong dependence of mode conversion on bend radius of the fibre (Gambling,W.A., Payne, D.N. and Matsumura,H., 1972) but it was subsequently discovered that this was largely due to distortion of the cladding since the fibre was wound on the supporting drums under tension (Gambling,W.A., Payne,D.N. and Matsumura,H.,1973a). An investigation of undistorted liquid-core fibres has produced some interesting results.

By adjusting launching conditions so that an input Gaussian beam excites mainly the HE_{11} mode, quasi-single-mode propagation has been observed in fibres of 57μm core diameter and in lengths of hundreds of metres. The launching source is a He/Ne laser operating at a wavelength of 0.633μm so that the degree of over-moding is indicated by the ratio core diameter/wavelength of 90 corresponding to a normalized frequency $v \simeq 130$. By changing the launching conditions higher-order modes can be launched and good agreement between theory and experiment is obtained for the output mode angular distribution for all modes up to HE_{17} (Gambling,W.A., Payne, D.N. and Matsumura,H., 1973b). These results indicate that the amount of scattering, particularly due to wall

imperfections and asymmetries in the core, are negligible over the lengths measured.

In straight liquid-core fibres it should therefore be possible to achieve propagation with only a small amount of mode conversion. However for laboratory measurements over appreciable lengths the fibres must be coiled on supporting drums and the resulting curvature of the fibre axis must inevitably produce some mode conversion and in order to estimate its magnitude and effect, as well as to differentiate between the effects of curvature and stress, an analysis has been made of optical propagation in a perfect, curved, cylindrical, multimode fibre.

Analyses of the mode conversion caused by wall imperfections have previously been reported (Marcuse,D., 1969; Gloge,D.,1972) and Marcatili (1969) has studied the effect of bends in waveguides of rectangular cross-section under the assumption that only TEM modes are excited. The analysis described here considers coupling due to bends in fibres of circular cross-section. For a beam incident on the fibre at normal incidence it has been shown theoretically (Snyder,A.W., 1969b) that only $HE_{1,m}$ modes are excited and this has been confirmed by experiment (Gambling,W.A.,Payne, D.N. and Matsumura,H., 1973b). The following analysis assumes that only $HE_{1,m}$ modes are launched and also that the difference between the refractive indices of core and cladding is small compared with unity, thus enabling the core mode approximation to be invoked.

2. FIELD ANALYSIS OF THE CURVED CYLINDRICAL FIBRE

The first step is to perform a field analysis from which coupling coefficients between the $HE_{1,m}$ modes and the $HE_{2,n}$ and $TE_{0,n}$ modes are derived. In order to describe the electromagnetic fields in a curved cylindrical dielectric waveguide the curvilinear cylindrical co-ordinates (r,θ,z) are used, as in Fig.1, where the longitudinal co-ordinate z is the distance along the curved axis of the waveguide and r,θ are polar co-ordinates in the plane normal to the curved axis. The incremental length of a ray in such a system is

$$(ds)^2 = (dr)^2 + r^2(d\theta)^2 + (1+\eta/R_o)^2(dz)^2 \qquad (1)$$

where $\eta = \eta(r,\theta) = r\cos\theta$ and R_o is the radius of curvature of the fibre axis. Making the usual assumption of a sinusoidal time dependence of angular frequency ω Maxwell's equations for the field components can be written:

$$\begin{aligned}
\frac{1}{r}\frac{\partial}{\partial\theta}(hE_z) - \frac{\partial}{\partial z}(E_\theta) &= -j\omega\mu hH_r \\
\frac{\partial}{\partial z}(E_r) - \frac{\partial}{\partial r}(hE_z) &= -j\omega\mu hH_\theta \\
\frac{1}{r}\frac{\partial}{\partial r}(rE_\theta) - \frac{1}{r}\frac{\partial}{\partial\theta}(E_r) &= -j\omega\mu H_z \qquad (2)\\
\frac{1}{r}\frac{\partial}{\partial\theta}(hH_z) - \frac{\partial}{\partial z}(H_\theta) &= -j\omega\epsilon hE_r \\
\frac{\partial}{\partial z}(H_r) - \frac{\partial}{\partial r}(hH_z) &= -j\omega\epsilon hE_\theta \\
\frac{1}{r}\frac{\partial}{\partial r}(rH_\theta) - \frac{1}{r}\frac{\partial}{\partial\theta}(H_r) &= -j\omega\epsilon E_z
\end{aligned}$$

where $$h = 1 + \eta/R_o \qquad (3)$$

The longitudinal components E_z and H_z can be written from eqn.(2) in terms of the transverse components

$$\begin{aligned}
j\omega\epsilon E_z &= \nabla_t\cdot(\bar{H}_t \times \bar{z}) \\
j\omega\mu H_z &= -\nabla_t\cdot(\bar{E}_t \times \bar{z})
\end{aligned} \qquad (4)$$

It may also be shown from eqn.(2) that

$$j\omega\epsilon \frac{\partial \bar{E}_t}{\partial z} = \nabla_t\left[h\nabla_t\cdot(\bar{H}_t \times \bar{z})\right] + \omega^2\mu\epsilon h(\bar{H}_t \times \bar{z})$$
$$j\omega\mu \frac{\partial \bar{H}_t}{\partial z} = -\nabla_t\left[h\nabla_t\cdot(\bar{E}_t \times \bar{z})\right] - \omega^2\mu\epsilon h(\bar{E}_t \times \bar{z}) \quad (5)$$

where $\bar{E}_t$, $\bar{H}_t$ are the electric and magnetic vectors in the transverse direction, respectively, ∇_t is the differential gradient operator operating on the transverse components and $\bar{z}$ is a unit vector.

Making the usual assumption of a small difference between the refractive indices (n_1, n_2) and dielectric constants (ϵ_1, ϵ_2) of the core and cladding, respectively, so that $\delta = 1 - (n_2/n_1)^2 << 1$ and assuming an infinitely thick cladding, the property of orthogonality of the fields gives:

$$\int_s \bar{e}_{\ell m} \times \bar{h}^*_{\ell' m'}\cdot\bar{z}\; r\, dr d\theta = \begin{cases} 1 & \ell, m = \ell', m' \\ 0 & \ell, m \neq \ell', m' \end{cases}$$
$$\bar{e}_{\ell m} = (\mu/\epsilon_1)^{\frac{1}{2}}\bar{h}_{\ell m} \times \bar{z} \quad (6)$$

where $\bar{e}_{\ell m}$, $\bar{h}_{\ell' m'}$ are the normalized eigenfunctions of modes ℓ, m; ℓ', m' of the transverse field, respectively.

The transverse electromagnetic field of the curved waveguide is now expanded in terms of the characteristic modes of the straight waveguide:

$$\bar{E}_t = \sum_{\ell=0}\sum_{m=0} E_{\ell m}\,\bar{e}_{\ell m}(r,\theta)$$
$$\bar{H}_t = \sum_{\ell=0}\sum_{m=0} H_{\ell m}\,\bar{h}_{\ell m}(r,\theta) \quad (7)$$

where $E_{\ell m}$ and $H_{\ell m}$ are the expansion coefficients and are functions of z. For clarity and ease of writing it is convenient to represent the mode designation ℓ, m by p; and ℓ', m' by q.

Substitution of eqn.(7) into eqn.(5), and using the orthogonality property as given by eqn.(6), results in the following coupled equations for $E_p(z)$ and $H_p(z)$:

$$\frac{\partial E_p}{\partial z} = -\sum_q A_{pq}H_q$$
$$\frac{\partial H_p}{\partial z} = -\sum_q B_{pq}E_q \quad (8)$$

where

$$A_{pq} = j\omega\epsilon_1\int_s h\bar{e}_q\cdot\bar{e}_p\, da - \frac{\epsilon_1}{j\omega\mu}\int_s \nabla_t\left(\frac{h}{\epsilon}\nabla_t\cdot\bar{e}_q\right)\cdot\bar{e}_p\, da$$
$$B_{pq} = j\omega\frac{\mu}{\epsilon_1}\int_s \epsilon\, h\bar{h}_q\cdot\bar{h}_p\, da - \frac{1}{j\omega\epsilon_1}\int_s \nabla_t(h\nabla_t\cdot\bar{h}_q)\cdot\bar{h}_p\, da \quad (9)$$

A_{pq} and B_{pq} are the coupling coefficients between modes p(i.e. ℓ, m) and q(ℓ', m').

For a weakly-guiding structure it is a straightforward matter to derive the self-coupling coefficients and the propagation constant β'_p of mode p is obtained from the square root of the product of the self-coupling coefficients giving

$$A_{pp} = j\omega(\mu\epsilon_1)^{\frac{1}{2}}\left\{1 - \left[\frac{u_p^2}{\alpha} + \frac{\epsilon_1}{\epsilon_2}\frac{(1-\alpha)w_p^2\theta_p^2}{\alpha}\right] / 2k^2\right\}$$
$$B_{pp} = j\omega(\mu\epsilon_1)^{\frac{1}{2}}\left(1 + \frac{1-\alpha}{\alpha}\theta_p^2 - u_p^2/2k^2\alpha\right) \quad (10)$$

where

$\theta_p = u_p/k$

$k = \rho\omega\sqrt{\mu\epsilon_1}$

ρ = core radius

$\alpha = K_\ell(w_p)K_{\ell\pm2}(w_p)/K^2_{\ell\pm1}(w_p)$

K_ℓ = modified Hankel function

w_p, u_p = eigenvalues which are related to the normalized frequency v as:

$$v^2 = (\rho\omega)^2\mu\epsilon_1\delta = u_p^2 + w_p^2 \tag{11}$$

The normalized propagation constant $\beta_p = \rho\beta'_p$ is given by

$$\begin{aligned}\beta_p &= jk\left[\left\{1 - \left[\frac{u_p^2}{\alpha} + \frac{\epsilon_1}{\epsilon_2}\left(\frac{1-\alpha}{\alpha}\right)w_p^2\theta_p^2\right]/2k^2\right\}\left(1 - u_p^2/2k^2\alpha + \frac{1-\alpha}{\alpha}\theta_p^2\right)\right]^{\frac{1}{2}} \\ &\simeq jk(1 - \theta_p^2/\alpha) \\ &\simeq jk(1 - \theta_p^2) \text{ far from cut-off}\end{aligned} \tag{12}$$

This result is identical to that for the propagation constant of a straight weakly-guiding fibre because the w_p are large except near cut-off.

If the fibre is excited by a Gaussian beam or a plane wave from a laser then only HE_{1m} modes are launched and this assumption will be followed here. Let the various quantities corresponding to the TE_{0m} modes be denoted by the subscript [0m] , those for the HE_{1m} modes by $\langle 1m\rangle$ and for the EH_{1m} modes by $\ll 1m\gg$. Since only one of the TE or TM sets of modes are coupled to the HE_{1m} modes only TE_{0m} modes will be considered, but similar results are obtained when coupling to the TM_{0m} modes takes place. Then, using eqn.(9), the coupling coefficients may be obtained and are given in eqns.(13) which are contained in the Appendix.

If the coupling coefficients for the curved fibre are studied it is seen that the $HE_{2,m} \Leftrightarrow TE_{0,m}$ modes are coupled to the $HE_{1,m}$ modes. In eqn.(13) the second term of $B_{\langle 1,m\rangle[0,n]}$ is neglected since $(1/2k^2) \ll 1$ and the following terms in the square brackets are all of the order of unity. (For the fibres with which we are concerned $\rho \sim 50\mu m$ for which $(1/2k^2) = 2\times10^{-6}$ and even when $\rho = 5\mu m$, which is very small for a multimode fibre $(1/2k^2) = 2\times10^{-4}$.) Similarly the coupling coefficients $A_{\langle 1,m\rangle\langle 1,n\rangle}$, $A_{\langle 1,m\rangle\ll 1,n\gg}$, $B_{\langle 1,m\rangle\langle 1,n\rangle}$ and $B_{\langle 1,m\rangle\ll 1,n\gg}$ can also be neglected since they are all small compared with the self-coupling coefficients of eqn.(10). As a result the form of coupling turns out to be very simple:

$$\begin{aligned}A_{\langle 1,m\rangle\langle 2,n\rangle} &= A_{\langle 1,m\rangle[0,n]} = B_{\langle 1,m\rangle\langle 2,n\rangle} = B_{\langle 1,m\rangle[0,n]} \\ &= \left(\frac{2jk/R_o}{\alpha_{\langle 1,m\rangle}\alpha_{q'}}\right)^{\frac{1}{2}} \cdot \frac{u_{\langle 1,m\rangle}u_{q'}}{(u_{\langle 1,m\rangle}^2 - u_{q'}^2)^2}\end{aligned} \tag{14}$$

where q' denotes the $HE_{2,m}$ and $TE_{0,m}$ modes.

Numerical values for the coupling coefficients have been evaluated and are given in Table 1 for a normalized frequency v=100 which is a typical value for a multimode fibre. The factor $2jk/R_o$ has been omitted from the Table. The coupling coefficients along a diagonal line are so much larger than the others that a coupling diagram, as in Fig.2, can be drawn.

It is interesting to compare this result with that for a straight waveguide having a wall fluctuation. By considering a slab waveguide with slightly distorted interfaces it has been shown (Marcuse, D., 1969) that in this case also coupling occurs mainly to nearest neighbours.

3. DISTRIBUTED ENERGY TRANSFER WITH THE HE_{11} MODE

In order to achieve maximum transmission distance and bandwidth in an optical fibre waveguide a laser source must be used and the input beam must be carefully controlled (Gambling,W.A., Payne, D.N. and Matsumura, H., 1972). A simple and convenient technique is to operate the laser in its lowest-order transverse (TEM_{oo}) mode in which case the spatial distribution of the beam is Gaussian and if it is launched into the core symmetrically then only $HE_{1,m}$ modes are set up in the core (Stern,R.J., Peace, M and

Dyott,R.B., 1970). Using Snyder's approximate field equations (Snyder,A.W. 1969 a and b) it is possible to develop an expression for the relative power $P_{l,m}$ coupled into the various $HE_{l,m}$ modes:

$$P_{l,m} = 2\left[\frac{U_m K_o(W_m)}{vK_1(W_m)} \frac{2\rho}{\omega_o}\left\{\int_o^1 \frac{J_o(U_m R)}{J_o(U_m)} \times \exp\left[-\frac{R^2}{(\omega_o/\rho)^2}\right] RdR + \int_1^\infty \frac{K_o(W_m R)}{K_o(W_m)} \times \exp\left[-\frac{R^2}{(\omega_o/\rho)^2}\right] RdR\right\}\right]^2 \quad (15)$$

where ω_o is the spot size of the input beam.

Values of $P_{l,m}$ have been calculated for a range of input beam widths assuming a typical normalized frequency of v=100 and are shown in Fig.3. It can be seen that for $\omega_o/\rho = 0.66$ as much as 97.3% of the input power is taken up by the HE_{11} mode and only 0.6% enters the HE_{12} mode. This condition is easy to achieve in practice (Gambling, W.A., Payne, D.N. and Matsumura,H., 1973b) and it will therefore be assumed in the following analysis that a virtually pure HE_{11} mode is launched into the fibre and the effect of the distributed coupling into the TE_{01} and HE_{21} modes will be considered.

From the coupling equations the following equations can be obtained:

$$\begin{aligned}
\frac{\partial E_{\langle 1,1\rangle}}{\partial z} &= -(A_{\langle 1,1\rangle\langle 1,1\rangle} H_{\langle 1,1\rangle} + A_{\langle 1,1\rangle\langle 2,1\rangle} H_{\langle 2,1\rangle} + A_{\langle 1,1\rangle[0,1]} H_{[0,1]}) \\
\frac{\partial E_{\langle 2,1\rangle}}{\partial z} &= -(A_{\langle 2,1\rangle\langle 1,1\rangle} H_{\langle 1,1\rangle} + A_{\langle 2,1\rangle\langle 2,1\rangle} H_{\langle 2,1\rangle}) \\
\frac{\partial E_{[0,1]}}{\partial z} &= -(A_{[0,1]\langle 1,1\rangle} H_{\langle 1,1\rangle} + A_{[0,1][0,1]} H_{[0,1]}) \\
\frac{\partial H_{\langle 1,1\rangle}}{\partial z} &= -(B_{\langle 1,1\rangle\langle 1,1\rangle} E_{\langle 1,1\rangle} + B_{\langle 1,1\rangle\langle 2,1\rangle} E_{\langle 2,1\rangle} + B_{\langle 1,1\rangle[0,1]} E_{[0,1]}) \\
\frac{\partial H_{\langle 2,1\rangle}}{\partial z} &= -(B_{\langle 2,1\rangle\langle 1,1\rangle} E_{\langle 1,1\rangle} + B_{\langle 2,1\rangle\langle 2,1\rangle} E_{\langle 2,1\rangle}) \\
\frac{\partial H_{[0,1]}}{\partial z} &= -(B_{[0,1]\langle 1,1\rangle} E_{\langle 1,1\rangle} + B_{[0,1][0,1]} E_{[0,1]})
\end{aligned} \quad (16)$$

where the coupling coefficients between the HE_{21} and TE_{01} modes are taken to be zero.

Now using eqns.(10) and (14) it is possible to simplify eqn.(16) to:

$$\begin{aligned}
\frac{\partial E_1}{\partial z} &= -A_{11}H_1 - A_{12}(H_2 + H_0) \\
\frac{\partial (E_2+E_0)}{\partial z} &= -2A_{12}H_1 - A_{22}(H_2 + H_0) \\
\frac{\partial H_1}{\partial z} &= -B_{11}E_1 - B_{12}(E_2 + E_0) \\
\frac{\partial (H_2+H_0)}{\partial z} &= -2B_{12}E_1 - A_{22}(E_2 + E_0)
\end{aligned} \quad (17)$$

where, again for simplification, the new suffixes 0,1,2 are used to represent, respectively, $[0,1]$, $\langle 1,1\rangle$ and $\langle 2,1\rangle$ that is they refer to the $TE_{0,1}$, $HE_{1,1}$ and $HE_{2,1}$ modes. For further simplification let

$$\begin{aligned}
E_2 + E_0 &= E_3 \\
H_2 + H_0 &= H_3 \\
\text{and write } E_i &= a_i + b_i \\
H_i &= a_i - b_i \quad \text{where } i=1,3
\end{aligned} \quad (18)$$

then

$$\begin{aligned}
\frac{\partial a_1}{\partial z} &= -A_{11}a_1 - A_{12}a_3 \\
\frac{\partial a_3}{\partial z} &= -2A_{12}a_1 - A_{22}a_3 \\
\frac{\partial b_1}{\partial z} &= A_{11}b_1 + A_{12}b_3 \\
\frac{\partial b_3}{\partial z} &= 2A_{12}b_1 + A_{22}b_3
\end{aligned} \tag{19}$$

The general solutions of eqn.(19) are as follows:

$$\begin{aligned}
a_1 &= (\lambda_1 + A_{22} - A_{12})C_1\exp\lambda_1 z + (\lambda_2 + A_{22} - A_{12})C_2\exp\lambda_2 z \\
a_3 &= (\lambda_1 + A_{11} - 2A_{12})C_1\exp\lambda_1 z + (\lambda_2 + A_{11} - 2A_{12})C_2\exp\lambda_2 z \\
b_1 &= (\beta_1 - A_{22} + A_{12})C_3\exp\beta_1 z + (\beta_2 - A_{22} + A_{12})C_4\exp\beta_2 z \\
b_3 &= (\beta_1 - A_{11} + 2A_{12})C_3\exp\beta_1 z + (\beta_2 - A_{11} + 2A_{12})C_4\exp\beta_2 z
\end{aligned} \tag{20}$$

where

$$\begin{aligned}
\left.\begin{matrix} 2\beta_1 \\ 2\beta_2 \end{matrix}\right\} &= (A_{11} + A_{22}) \pm \left[(A_{11} - A_{22})^2 + 8A_{12}^2\right]^{\frac{1}{2}} \\
&= (A_{11} + A_{22}) \pm A_f \\
\left.\begin{matrix} 2\lambda_1 \\ 2\lambda_2 \end{matrix}\right\} &= -(A_{11} + A_{22}) \pm \left[(A_{11} - A_{22})^2 + 8A_{12}^2\right]^{\frac{1}{2}} \\
&= -(A_{11} + A_{22}) \pm A_f
\end{aligned} \tag{21}$$

and the constants C_1 to C_4 are determined by the boundary conditions. From eqns.(10), (14), (20) and (21) it can be shown that the quantity b represents backward waves in the fibre but these are negligible compared with forward-travelling waves since the forward HE_{11} mode must predominate at the input, so that $B_1=b_2=0$ at $z=0$ and hence $C_3=C_4=0$. The b terms can thus be neglected and inserting the boundary conditions, $a_1=1$, $a_3=0$ at $z=0$ into eqn.(20) gives:

$$\begin{aligned}
C_1 &= \frac{\lambda_2 + A_{11} - 2A_{12}}{(\lambda_1-\lambda_2)(A_{11}-A_{22}-A_{12})} \\
-C_2 &= \frac{\lambda_1 + A_{11} - 2A_{12}}{(\lambda_1-\lambda_2)(A_{11}-A_{22}-A_{12})}
\end{aligned} \tag{22}$$

Finally the fields in the curved waveguide are:

$$\begin{aligned}
\bar{E}_t A_f &= \left[(\lambda_1 + A_{11})\exp\lambda_2 z - (\lambda_2 + A_{11})\exp\lambda_1 z\right]\bar{e}_1 \\
&\quad + A_{12}(\exp\lambda_2 z - \exp\lambda_1 z)(\bar{e}_o + \bar{e}_2) \\
\bar{H}_t A_f &= \left[(\lambda_1 + A_{11})\exp\lambda_2 z - (\lambda_2 + A_{11})\exp\lambda_1 z\right]\bar{h}_1 \\
&\quad + A_{12}(\exp\lambda_2 z - \exp\lambda_1 z)(\bar{h}_o + \bar{h}_2)
\end{aligned} \tag{23}$$

One check on this result is to let $R_o \to \infty$ when the result obtained is:

$$\begin{aligned}
\bar{E}_t &= \bar{e}_1 \exp\left[-j\omega(\mu\epsilon_1)^{\frac{1}{2}}(1 - \tfrac{1}{2}\theta_p^2)z\right] \\
\bar{H}_t &= \bar{h}_1 \exp\left[-j\omega(\mu\epsilon_1)^{\frac{1}{2}}(1 - \tfrac{1}{2}\theta_p^2)z\right]
\end{aligned} \tag{24}$$

Eqn.(24) is, as expected, identical with that obtained from the analysis of a straight, weakly guiding waveguide, i.e. with $\delta \ll 1$.

Having obtained expressions for the fields in the curved waveguide it is possible to study the energy transfer between modes by calculating the flux density from the time-averaged axial component of the Poynting vector, $S_z = \frac{1}{2}\mathrm{Re}(\bar{E} \times \bar{H}^*)_z$ (25)

As may be seen from Fig.1 the energy distribution is expected to be symmetrical about the $\theta=0,\pi$ direction so that the energy flux density will be found for the values $\theta=0$ and $\theta=\pi$, i.e. in the plane of curvature. In the following the primes on symbols denote real parts, thus $A'_{11} = \omega(\mu\epsilon_1)^{\frac{1}{2}}(1 - \frac{1}{2}\theta_p^2)$

Now in those longitudinal positions where $(\lambda'_1 - \lambda'_2)z = 2m\pi$ where m is an integer then

$$S_z = (\epsilon_1/\mu)^{\frac{1}{2}} e_1^2 \qquad (26)$$

and the energy distribution corresponds to that of the $HE_{1,1}$ mode.

On the other hand when $(\lambda'_1 - \lambda'_2)z = (2m + 1)\pi$ then

$$S_z = (\epsilon_1/\mu)^{\frac{1}{2}}(\lambda'_1-\lambda'_2)^{-2}\left[(\lambda'_1+\lambda'_2+2A'_{11})e_1 \pm 2A'_{12}(e_o+e_2)\right]^2 \qquad (29)$$

Eqn.(29) shows that in a fibre which is not too sharply curved the point of maximum energy density shifts away from the centre of curvature by an amount which depends on the bend radius. The energy distribution in the $\theta=0,\pi$ direction, for a normalized frequency $v=100$ and normalized radius of curvature $R_o/\rho = 5\times10^4$, for four values of $(\lambda'_1-\lambda'_2)z$, is shown in Fig.4. It can be seen that starting from the HE_{11} distribution an outward shift occurs as coupling to the HE_{21} and TE_{01} modes takes place followed by a complete transfer back to the HE_{11} mode again.

The total power density P_t in all modes can be obtained using eqn.(25) by integrating over the entire cross-section from r=0 to $r=\infty$, thus

$$P_t = \int S_z r\, dr d\theta \qquad (30)$$

In this way the rate of power transfer from the HE_{11} mode to the HE_{21} and TE_{01} modes can be derived:

$$P_t = P_{\langle 11\rangle} + P_{(\langle 21\rangle + [01])} = P_1 + P_{2,0} \qquad (31)$$

where

$$P_1 = (\lambda'_1-\lambda'_2)^{-2}\left[(\lambda'_1+A'_{11})^2 + (\lambda'_2+A'_{11})^2 - 2(\lambda'_1+A'_{11})(\lambda'_2+A'_{11})\cos(\lambda'_1-\lambda'_2)z\right] \qquad (32)$$

$$P_{2,0} = \frac{4(A'_{12})^2}{(\lambda'_1-\lambda'_2)^2}\left[1 - \cos(\lambda'_1-\lambda'_2)z\right]$$

and

$$P_1 + P_{2,0} = 1 \qquad (33)$$

These equations confirm that $P_{2,0}$ is zero at $(\lambda'_1-\lambda'_2)z = 2m\pi$ and a maximum at $(\lambda'_1-\lambda'_2)z$ for various normalized radii of curvature (R_o/ρ) at a normalized frequency $v=100$. Taking one case as an example, if the core diameter is 50μm and the bend radius is 25cm then $R_o/\rho = 10^4$ and $P_{2,0}$ rises to a maximum value of $0.75P_t$. For $R_o>2m$ the power transfer is negligible and the fibre behaves as a straight waveguide. The power transfer is shown in Fig.5(b) to become greater as the normalized frequency is increased.

It is also useful to compute the ratio Q of the total power which is carried in the core and from eqns.(23) and (30) it is possible to show that:

$$Q = \left[1 - \left(\frac{u_1}{v}\right)^2(1-\alpha_1^{-1})\right] - 4A'^2_{12}(\lambda'_1-\lambda'_2)^{-2}\left[1 - \cos(\lambda'_1-\lambda'_2)z\right]\left[\left(\frac{u_2}{v}\right)^2(1-\alpha_2^{-1}) - \left(\frac{u_1}{v}\right)^2(1-\alpha_1^{-1})\right] \qquad (34)$$

The variation of Q with z and v is shown in Fig.6(a) and (b). Q is a minimum at $(\lambda'_1-\lambda'_2)z = (2m+1)\pi$ and increases with v, as would be expected from the mode conversion results of Fig.5. In order to show the effect more clearly Fig.6(a) is calculated for $v=20$. From the value of Q at z=0 it is found that the proportion of the HE_{11} mode power which is carried in the cladding is 0.06%. The minimum value of Q is given as a function of v in Fig.6(b) and it may be seen that when v exceeds about 80 the penetration of the fields into the cladding is negligible.

4. EXPERIMENT

It might be expected that there would be some difficulty in observing experimentally the effects predicted in the above theory because in most fibres propagation is dominated by imperfections in the core/cladding interface, inhomogeneities, stress and birefringence. However, as mentioned earlier, core inhomogeneities and birefringence do not affect a liquid-core fibre, while by producing the cladding capillary on a precision fibre-drawing machine the interface can be made almost perfect so that, as we have already shown (Gambling,W.A. Payne,D.N., and Matsumura,H., 1973b), discrete mode propagation over appreciable lengths can be achieved if care is taken to avoid stressing the fibre in any way.

Experiments have therefore been performed on a liquid-core fibre consisting of hexachlorobuta-1,3-diene in Chance-Pilkington MEl glass tubing. The refractive indices of core and cladding, respectively, are 1.557 and 1.485 at a wavelength of 0.633μm giving a numerical aperture of 0.45. The core diameter was 57μm corresponding to a normalized frequency of v=125, so that the fibre is capable of supporting roughly 7,800 modes. A Gaussian beam from a helium/neon laser operating in a single, TEM_{00}, transverse mode was launched along the axis of various lengths of fibre up to 50m, but confirmatory checks were also made over 125m. With the lenses available the nearest it was possible to get to the optimum beam width for the fibre was ω_o/ρ =0.86 (instead of 0.66) so that about 90% of the input power entered the HE_{11} mode. Typical results are shown in Fig.7 for a fibre coiled loosely in a diameter of about 11cm. A pure HE_{11} mode is seen at (a) and this has been confirmed (Gambling,W.A., Payne,D.N. and Matsumura,H. 1973b) by measurement of the radial intensity distribution and the angular width of the pattern. Figs.7(b) to (e) were obtained by progressively shortening the fibre and show clearly the development of the TE_{01} and HE_{21} modes and their decay again so that the pure HE_{11} pattern is repeated. The shortening of the fibre between (a) and (e) was less than 1mm as predicted by the theory. By increasing the radius of curvature to R_o=100cm the periodic coupling length increased to 1.4cm.

Despite the low attenuation of the fibre, namely 40dB/km at the measurement wavelength of 0.633μm (5.8dB/km at 1.06μm) there was just sufficient light scattering to enable the beam locus to be observed under a microscope. The beam locus in Fig.8(a) is along the axis of the core at a position corresponding to the HE_{11} mode while Fig.8(b) was taken midway between two HE_{11} positions and the beam has now moved close to the core boundary on the outside of the curve. The periodic length measured by traversing the microscope along the fibre agrees with that found by shortening it. The observations show that the beam in a curved fibre follows an undulating path, moving from the axis to the outside of the bend and back again.

Confirmation of Snyder's (1969b) statement that only HE_{1m} modes are launched on a fibre by a Gaussian beam at normal incidence is given by the far-field patterns in Fig.9(a) and (b) which were obtained for a few metres length of straight fibre at two different ratios ω_o/ρ . Modes up to $HE_{1,10}$ can be clearly seen.

It was found that the simple mode pattern and the periodic coupling were destroyed when excessive mode conversion was caused by squeezing, and thus distorting,the fibre and by winding it under tension on a supporting drum.

5. CONCLUSIONS

By expanding the electromagnetic fields along a curved multimode cladded fibre in terms of the characteristic modes of a straight fibre the coupling coefficients between the HE_{1m} and other modes have been derived. It is found that coupling occurs mainly to $HE_{2,(m-1)}$; $TE_{0,(m-1)}$; $HE_{2,m}$ and $TE_{0,m}$ modes. In particular the analysis predicts a periodic coupling between the HE_{11} mode and the HE_{21} and TE_{01} modes and this has been confirmed experimentally by observation in the longitudinal direction of the far-field output pattern as the fibre length is changed and in the transverse direction of the beam 1 us. The experiments thus not only support the theory but indicate that in an unstressed fibre the amount of mode conversion due to wall imperfections, inhomogeneities and scattering is negligible.

6. REFERENCES

Gambling,W.A., Dakin,J.P., Payne,D.N. and Sunak H.R.D.,1972,'Propagation model for multimode optical-fibre waveguide', Electronics Letters, 8, pp260-262.

Gambling,W.A., Payne, D.N. and Matsumura,H., 1972,'Gigahertz bandwidths in multimode, liquid-core, optical fibre waveguide', Optics Communications, 6,pp 235-238.

Gambling,W.A., Payne,D.N. and Matsumura,H.,1973a,'Single-mode propagation in multimode fibres', paper presented at 1st National Quantum Electronics Conference, Manchester.

Gambling,W.A., Payne,D.N. and Matsumura,H., 1973b,'Mode excitation in a multimode optical-fibre waveguide', Electronics Letters, 9, pp412-414.

Gloge, D.,1972,'Optical power flow in multimode fibre', B.S.T.J., 51, pp1767-1783.

Marcatili, E.A.J., 1969, 'Bends in optical dielectric guides', B.S.T.J., 48, pp2103-2132.

Marcuse, D., 1969, 'Mode conversion caused by surface imperfections of a dielectric slab waveguide', B.S.T.J., 48, pp3187-3215.

Payne, D.N. and Gambling,W.A., 1973, 'The preparation of multimode glass- and liquid-core optical fibres', Opto-electronics, 5, pp297-307.

Snyder,A.W., 1969a,'Asymptotic expressions for eigenfunctions and eigenvalues of a dielectric or optical waveguide', IEEE Trans MTT-17, pp1130-1138.

Snyder,A.W., 1969b, 'Excitation and scattering of modes on a dielectric or optical fibre',IEEE Trans. MTT-17, pp1138-1144.

Stern,R.J., Peace,M. and Dyott,R.B.,1970, 'Launching into optical fibre waveguide', Electronics Letters, 6, pp160-162.

APPENDIX - EQUATION 13

$$A_{\langle l,m\rangle\langle l,n\rangle} = \frac{j}{k\rho\left(a_{\langle l,m\rangle}a_{\langle l,n\rangle}\right)^{\frac{1}{2}}} \frac{u_{\langle l,m\rangle}u_{\langle l,n\rangle}}{u^2_{\langle l,m\rangle} - u^2_{\langle l,n\rangle}} \left(\frac{w_{\langle l,n\rangle}K_{\langle l,n\rangle}}{K_{\langle 0,n\rangle}} - \frac{w_{\langle l,m\rangle}K_{\langle l,m\rangle}}{K_{\langle 0,m\rangle}} \right) + O(\delta)$$

$$A_{\langle l,m\rangle\langle l,n\rangle} = A_{\langle l,n\rangle\langle l,m\rangle}$$

$$= \frac{-j}{k\rho\left(a_{\langle l,m\rangle}a_{\langle l,n\rangle}\right)^{\frac{1}{2}}} \frac{u_{\langle l,m\rangle}u_{\langle l,n\rangle}}{u^2_{\langle l,m\rangle} - u^2_{\langle l,n\rangle}} \left(\frac{w_{\langle l,n\rangle}K_{\langle l,n\rangle}}{K_{\langle 2,n\rangle}} - \frac{w_{\langle l,m\rangle}K_{\langle l,m\rangle}}{K_{\langle 0,m\rangle}} \right) + O(\delta)$$

$$A_{\langle l,m\rangle\langle 2,n\rangle} = A_{\langle 2,m\rangle\langle l,n\rangle}$$

$$= \frac{2jk}{R_0\left(a_{\langle l,m\rangle}a_{\langle 2,n\rangle}\right)^{\frac{1}{2}}} \frac{u_{\langle l,m\rangle}u_{\langle 2,n\rangle}}{\left(u^2_{\langle l,m\rangle} - u^2_{\langle 2,n\rangle}\right)^2}$$

$$A_{\langle l,m\rangle[0,n]} = A_{[0,n]\langle l,m\rangle}$$

$$= \frac{2jk}{R_0 (a_{\langle 1,m\rangle} a_{[0,n]})^{\frac{1}{2}}} \frac{u_{\langle 1,m\rangle} u_{[0,n]}}{(u^2_{\langle 1,m\rangle} - u^2_{[0,n]})^2}$$

$$B_{\langle 1,m\rangle\langle 1,n\rangle} = \frac{j}{k\rho (a_{\langle 1,m\rangle} a_{\langle 1,n\rangle})^{\frac{1}{2}}} \frac{u_{\langle 1,m\rangle} u_{\langle 1,n\rangle}}{u^2_{\langle 1,m\rangle} - u^2_{\langle 1,n\rangle}} \left(\frac{w_{\langle 1,n\rangle} K_{\langle 1,n\rangle}}{K_{\langle 0,n\rangle}} - \frac{w_{\langle 1,m\rangle} K_{\langle 1,m\rangle}}{K_{\langle 0,m\rangle}} \right)$$

$$B_{\langle 1,m\rangle\langle 1,n\rangle} = B_{\langle 1,n\rangle\langle 1,m\rangle}$$

$$= \frac{j}{k\rho (a_{\langle 1,m\rangle} a_{\langle 1,n\rangle})^{\frac{1}{2}}} \frac{u_{\langle 1,m\rangle} u_{\langle 1,n\rangle}}{u^2_{\langle 1,m\rangle} - u^2_{\langle 1,n\rangle}} \left(\frac{w_{\langle 1,n\rangle} K_{\langle 1,n\rangle}}{K_{\langle 2,n\rangle}} - \frac{w_{\langle 1,m\rangle} K_{\langle 1,m\rangle}}{K_{\langle 0,m\rangle}} \right)$$

$$B_{\langle 1,m\rangle\langle 2,n\rangle} = B_{\langle 2,n\rangle\langle 1,m\rangle}$$

$$= \frac{2jk}{R_0 (a_{\langle 1,m\rangle} a_{\langle 2,n\rangle})^{\frac{1}{2}}} \frac{u_{\langle 1,m\rangle} u_{\langle 2,n\rangle}}{(u^2_{\langle 1,m\rangle} - u^2_{\langle 2,n\rangle})^2} + O(\delta)$$

$$B_{\langle 1,m\rangle[0,n]} = B_{[0,n]\langle 1,m\rangle}$$

$$= \frac{2jk}{R_0 (a_{\langle 1,m\rangle} a_{[0,n]})^{\frac{1}{2}}} \frac{u_{\langle 1,m\rangle} u_{[0,n]}}{(u^2_{\langle 1,m\rangle} - u^2_{[0,n]})^2} \left\{ 1 + \frac{1}{2k^2} \left[\left(\frac{w_{[0,n]} K_{[0,n]}}{K_{[1,n]}} - \frac{w_{\langle 1,m\rangle} K_{\langle 1,m\rangle}}{K_{\langle 0,m\rangle}} \right) (u^2_{\langle 1,m\rangle} - u^2_{[0,n]}) \right.\right.$$

$$\left.\left. - \frac{2w_{[0,n]} K_{[0,n]} w_{\langle 1,m\rangle} K_{\langle 1,m\rangle}}{K_{\langle 0,m\rangle} K_{[1,n]}} - \frac{u^2_{\langle 1,m\rangle} u^2_{[0,n]} - w^2_{\langle 1,m\rangle} w^2_{[0,n]}}{v^2} \right] \right\} + O(\delta)$$

where $O(\delta)$ is small compared with the other terms.

TABLE 1

Coefficients of coupling from the $HE_{1,m}$ modes to the $HE_{2,n}$ and $TE_{0,n}$ modes

$HE_{1,m}$ \ $HE_{2,n} + TE_{0,n}$	n = 1	2	3	4	5	6	7	8
m = 1	1.2 E-1	9.1 E-3	2.6 E-3	1.1 E-3	5.7 E-4	3.3 E-4	2.1 E-4	1.4 E-4
2	8.6 E-2	1.1 E-1	1.1 E-2	3.4 E-3	1.6 E-3	8.7 E-4	5.3 E-4	3.5 E-4
3	9.2 E-3	9.3 E-2	1.1 E-1	1.1 E-2	3.7 E-3	1.8 E-3	1.0 E-3	6.4 E-4
4	3.0 E-3	1.0 E-2	9.6 E-2	1.1 E-1	1.1 E-2	3.9 E-3	1.9 E-3	1.1 E-3
5	1.3 E-3	3.5 E-3	1.1 E-2	9.7 E-2	1.1 E-1	1.1 E-2	3.9 E-3	1.9 E-3
6	7.2 E-4	1.7 E-3	3.7 E-3	1.1 E-2	9.8 E-2	1.1 E-1	1.1 E-2	4.0 E-3
7	4.3 E-4	9.4 E-4	1.8 E-3	3.8 E-3	1.1 E-2	9.9 E-2	1.1 E-1	1.1 E-2
8	2.8 E-4	5.8 E-4	1.0 E-3	1.9 E-3	3.9 E-3	1.1 E-2	9.9 E-2	1.0 E-1
9	1.9 E-4	3.9 E-3	6.6 E-4	1.1 E-3	1.9 E-2	4.0 E-3	1.1 E-2	1.0 E-1

In the table E-3 denotes $\times 10^{-3}$ and the factor $(2jk/R_0)$ has been omitted

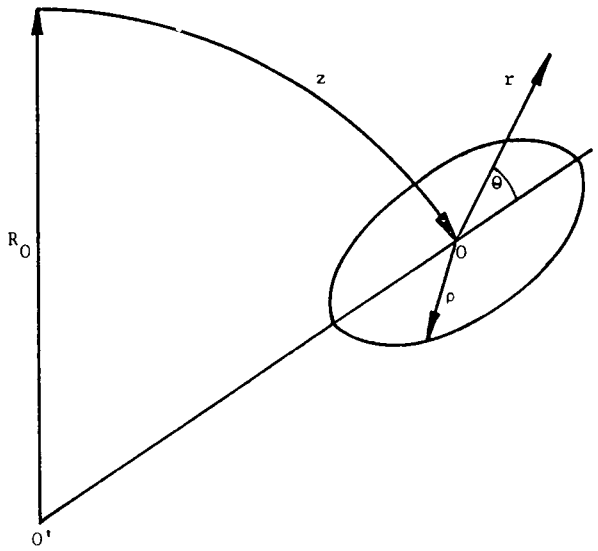

Fig.1 Toroidal co-ordinates used in the analysis of the curved waveguide

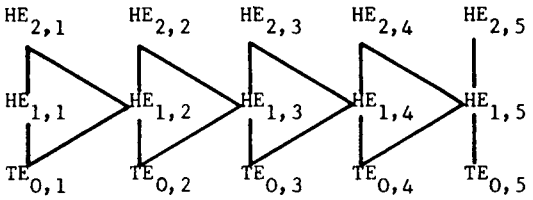

Fig.2 Diagram showing coupling between the $HE_{1,m}$ modes and the $HE_{2,n}$ and $TE_{0,n}$ modes

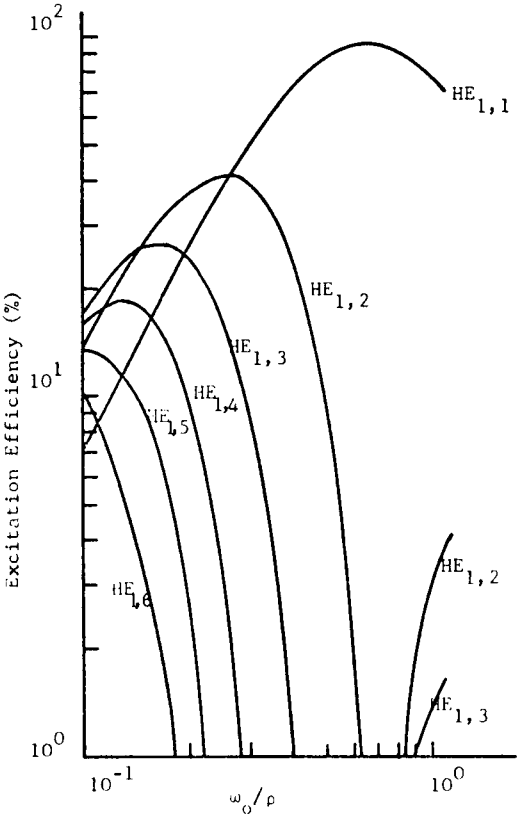

Fig.3 Theoretical excitation efficiency at normal incidence as a function of the normalized spot size of the input Gaussian beam for a normalized frequency v = 120

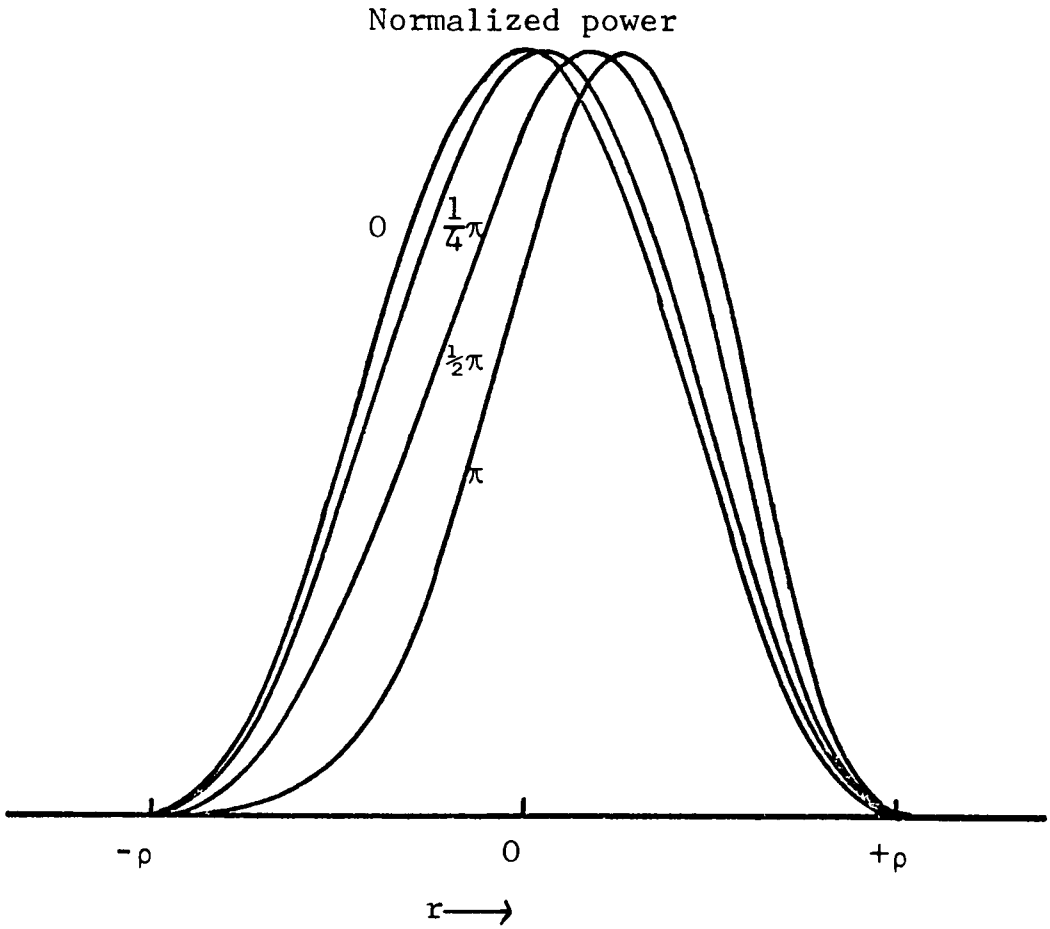

Fig.4 Transverse intensity distribution in the plane of curvature ($\theta = 0, \pi$) of the curved fibre for $R_0/\rho = 5 \times 10^4$ and for various values of $(\lambda_1' - \lambda_2')z$

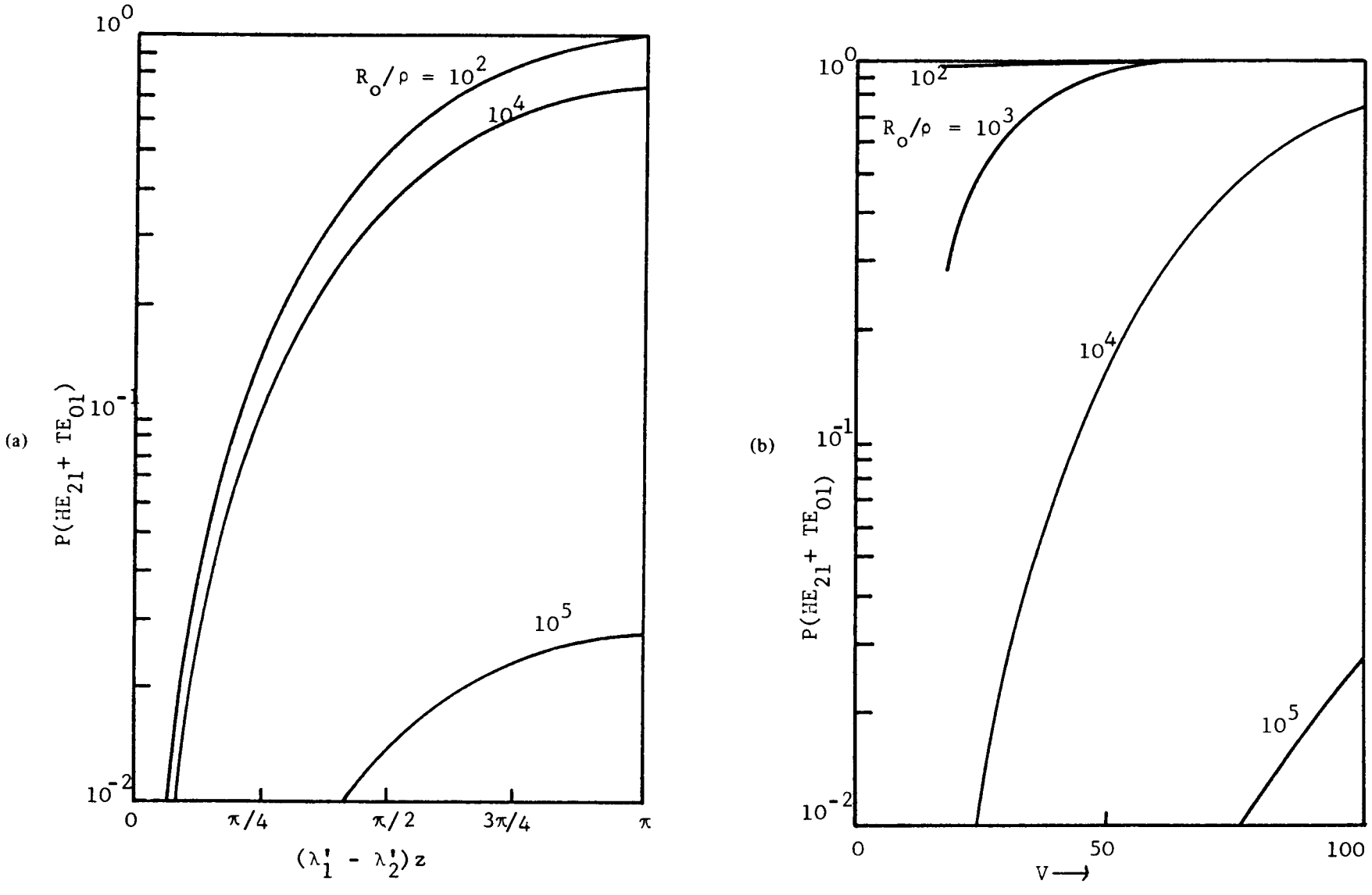

Fig.5 Power transfer to $HE_{2,1}$ and $TE_{0,1}$ modes as a function of
(a) normalized fibre length $(\lambda_1' - \lambda_2')z$ at $v = 100$, and
(b) normalized frequency v at $(\lambda_1' - \lambda_2')z = \pi$ for various values of R_0/ρ

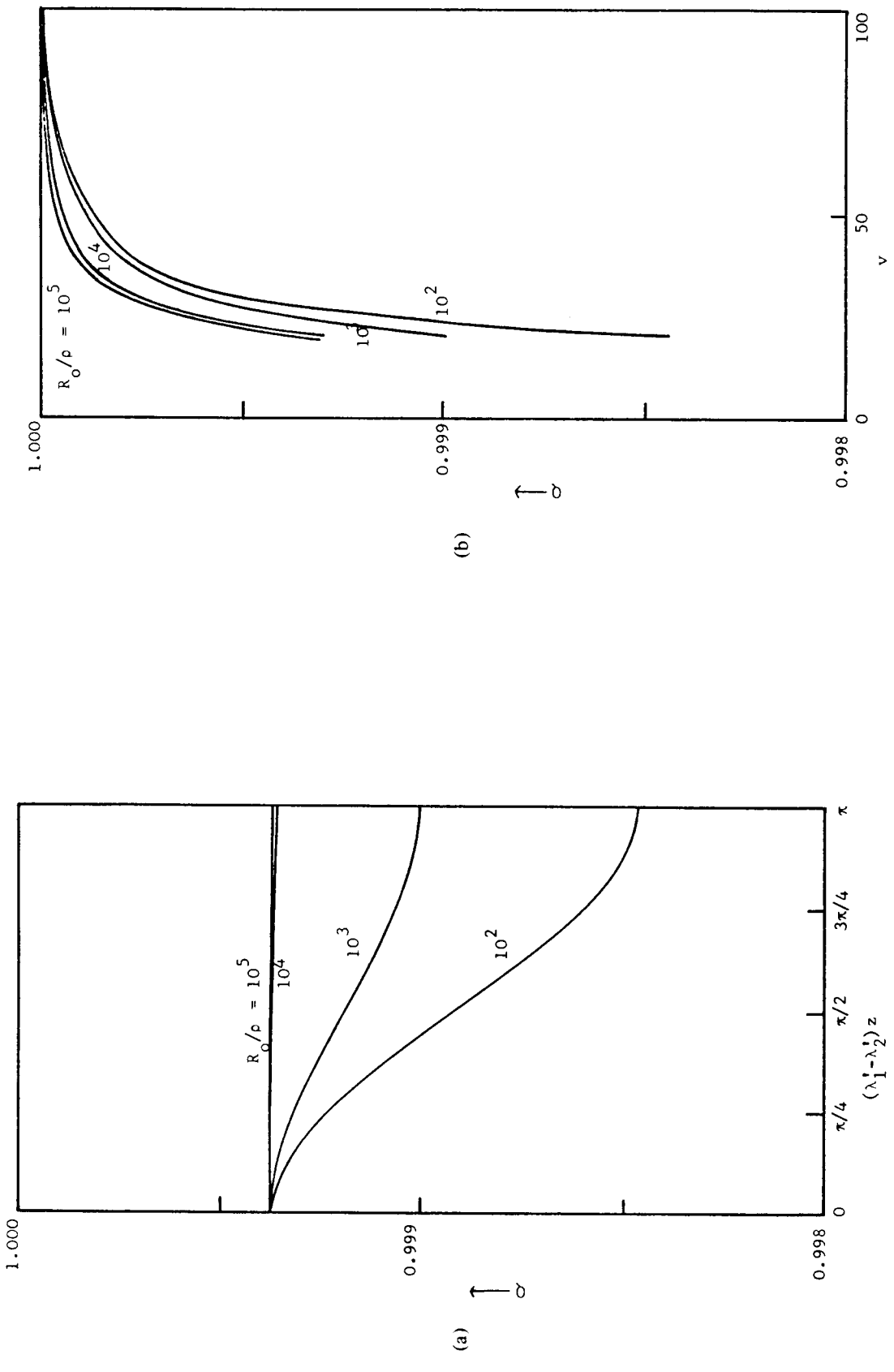

Fig.6 Ratio of the power contained within the core to the total power transmitted along the fibre as a function of
(a) normalized length of fibre $(\lambda_1' - \lambda_2')z$ at $v = 20$ and
(b) normalized frequency at $(\lambda_1' - \lambda_2')z = \pi$ for various values of R_0/ρ

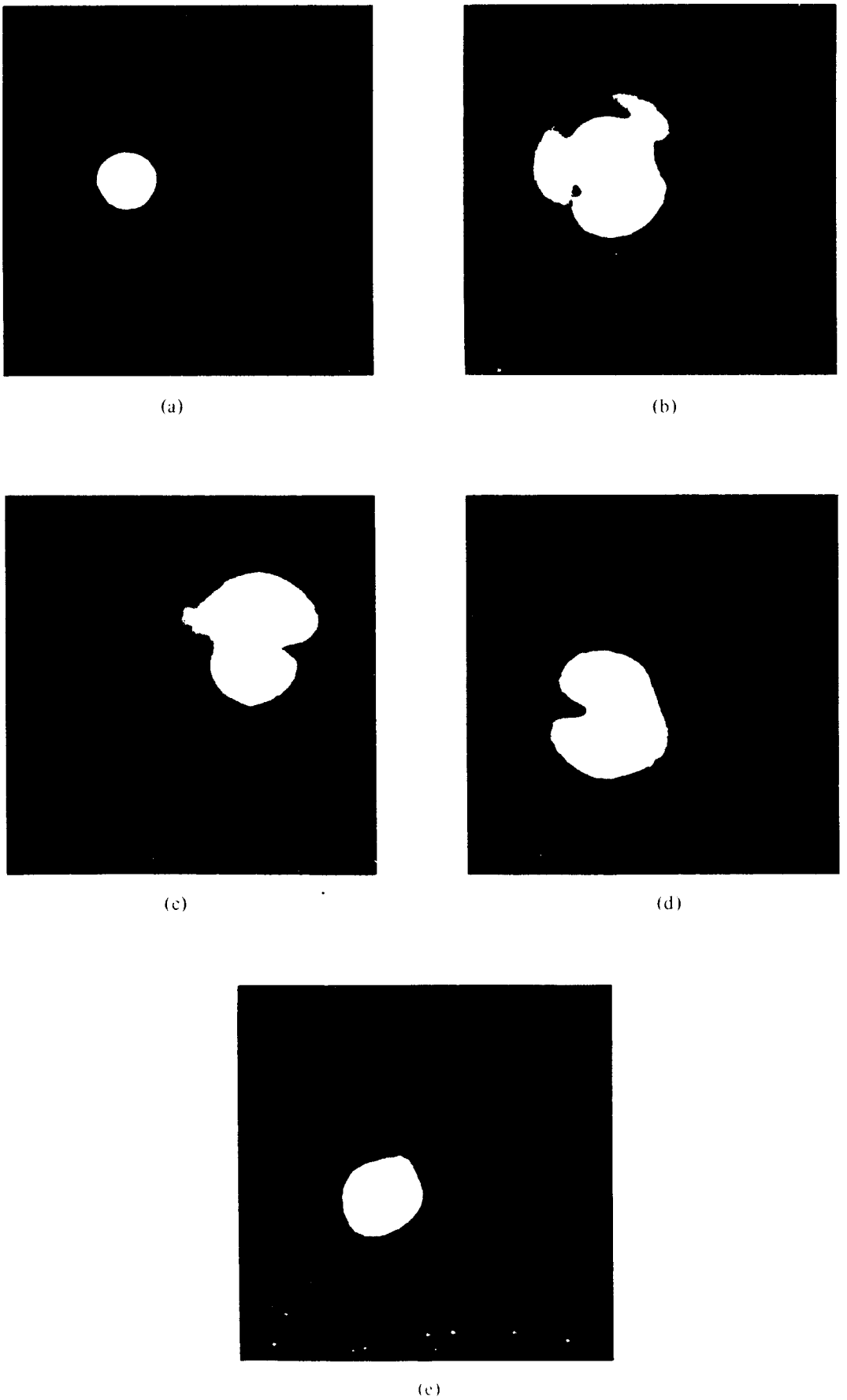

Fig.7 Far-field output patterns transmitted through progressively shorter lengths of curved fibre of 57μm core diameter. The normalized input spot size is about 0.86. The difference in length between (a) and (e) is less than 1 mm

(a) (b)

Fig.8 The locus of the beam in a curved fibre undulates periodically between the positions shown in (a) and (b). Position (a) corresponds to a pure HE_{11} mode and (b) to a combination of low-order modes

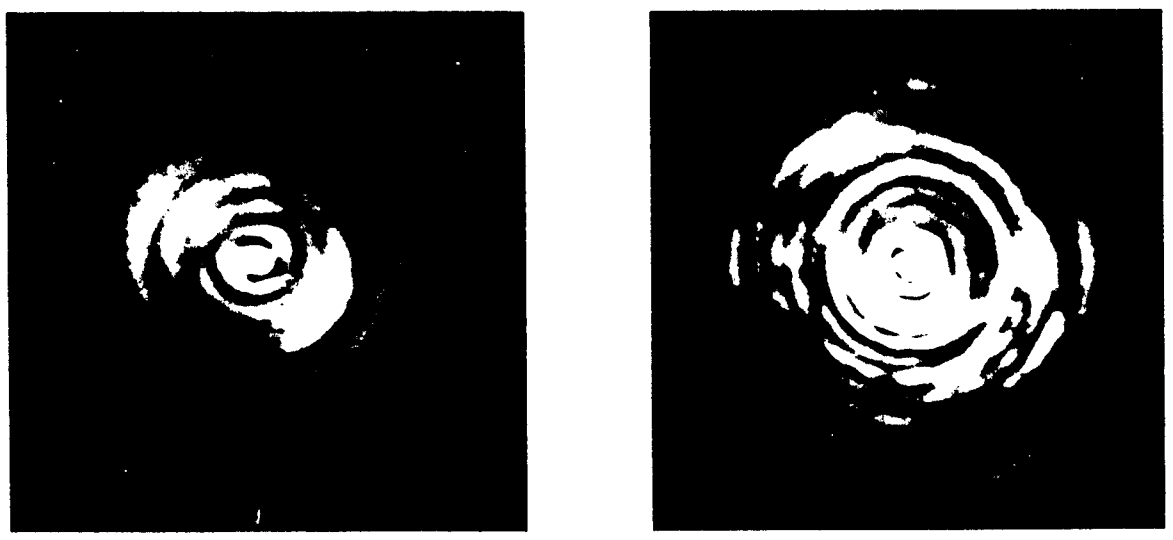

(a) (b)

Fig.9 Far-field output patterns from a straight fibre for a Gaussian input beam of normalized input spot size ω_0/ρ = 0.134(a) and 0.044(b) showing HE_{1m} modes for values of m up to 10